

## Analysis of the Effect Variation of Sides Racing Bike Helmets on Flow Characteristics Using CFD

Syamsuri<sup>1\*</sup>, Zain Lillahulhaq<sup>2</sup>, M. Mufarrichi<sup>3</sup>

<sup>1,2,3</sup>Department Mechanical Engineering, Institut Teknologi Adhi Tama Surabaya, Indonesia

\*Email: [syamsuri@itats.ac.id](mailto:syamsuri@itats.ac.id)

### Abstract

*The selection of materials and aerodynamic design forms needs to be considered in designing a comfortable helmet. This research aims to determine the effect of variations in helmet models on the drag force at a certain Reynold number. The emergence of the drag force on the helmet causes a compressive force, which causes the rider discomfort when driving at high speeds. This research was conducted on 4 variations of helmet models consisting of 1 time-trial type helmet as a reference and 3 other helmets which were developed from the basic model. This simulation was conducted in a 2D helmet model at  $Re\ 7.14 \times 10^4$ ,  $1.00 \times 10^5$ , and  $1.16 \times 10^5$ . In this study, Turbulence Intensity was varied as 0.1%, 0.2%, and 1%. The results are shown through the drag coefficient's value and visualization of streamlined flow. The results showed that the 2D simulation on the helmet produced a lower error by using Set Up Turbulence Intensity 0.1%. The emergence of the Oscillating Karman vortex in large size indicates the higher the drag force that occurs on the helmet. In this study, helmet type 3, with a trailing edge and has a smooth curve, has the lowest drag force at  $Re\ 1.16 \times 10^5$  with a drag coefficient value of around 0.38.*

**Keywords:** cfd, drag coefficient, racing bike helmet, vortex

### Abstrak

*Pemilihan bahan dan bentuk desain yang aerodinamis menjadi hal yang perlu diperhatikan dalam merancang suatu helm yang nyaman. Munculnya gaya drag pada helm menyebabkan munculnya gaya tekan pada helm yang menyebabkan rasa tidak nyaman pada pengendara saat melaju pada kecepatan tinggi. Penelitian ini dilakukan pada 4 variasi model helm yang terdiri dari 1 helm tipe time-trial sebagai acuan dan 3 helm lain yang dikembangkan dari model dasar. Penelitian ini dilakukan dengan menggunakan model helm 2D yang disimulasikan pada  $Re\ 7.14 \times 10^4$ ,  $1.00 \times 10^5$  dan  $1.16 \times 10^5$ . Penelitian ini juga memvariasikan set up Turbulence Intensity sebesar 0.1%, 0.2% dan 1%. Hasil simulasi akan di tunjukan melalui nilai koefisien drag dan visualisasi aliran streamline. Hasil penelitian menunjukkan bahwa simulasi 2D pada helm menghasilkan eror yang rendah dengan menggan menggunakan Set Up Turbulence Intensity 0.1%. Munculnya Oscillating Karman vortex dalam ukuran besar mengindikasikan semakin tingginya gaya drag yang terjadi pada helm. Pada penelitian ini helm tipe 3 dengan trailing edge dan lekukan yang halus memiliki gaya drag paling rendah pada  $Re\ 1.16 \times 10^5$  dengan nilai Koefisien drag sekitar 0.38.*

**Kata Kunci:** cfd, koefisien hambat, helm sepeda balap, vortex

## 1. Introduction

Cycling is a popular sport as well as a practical means of transportation. Cycling has become a popular sport, especially since the Covid-19 virus hit Indonesia. Public interest in cycling, both indoor and outdoor, has increased by 15% in various countries [1]. The use of bicycles as a mode of transportation can increase the risk of accidents and injuries to bicycle users. To protect themselves from possible injuries, cyclists equip themselves with

helmets and elbow and knee protectors. However, currently, accidents that occur in the use of bicycles have not become an issue that is considered important in Indonesia. Whereas traffic accidents while driving are the main cause of head injuries treated in the emergency department by 60% [2]. The percentage of cyclists' involvement in traffic accidents is very low compared to motor vehicles. Accidents involving cyclists continue to increase along with the increase in the number of

DOI: <http://dx.doi.org/10.24127/trb.v13i1.2699>

Received June 29, 2023; Received in revised form December 28, 2023; Accepted January 10, 2024

Available online June 30, 2024

20



cyclists [3]. In addition, during the COVID-19 pandemic, an increase in cycling enthusiasts and caused an increase in traffic accidents involving cyclists up to 28.4% [4]. The majority of accidents experienced by cyclists can be caused by violating a red light when crossing a road intersection [5], not using a proper helmet [6], and being in a blind spot by another vehicle when turning over [7]. Several countries have implemented mandatory the using of helmet to reduce the possibility of serious injury to cyclists [8]. The use of a helmet can reduce the likelihood of severe head injuries by up to 20% [9].

Helmets used by cyclists must have a high level of comfort, light, have good air circulation, and have the strength to withstand external forces. The use of composite materials as raw materials for manufacture aims to get a helmet that is strong and lightweight. The material commonly used as raw material for making helmets is thermoplastic woven carbon/Elium (WEL) composite. The inner support frame of the helmet is made of Carbon/Epoxy which is not able to absorb impact energy. When subjected to an impact, the supporting framework layer will break and can cause internal injuries to the head. Helmets made of WEL material have the advantage of being safe, able to absorb energy, and resistant to mechanical damage due to external forces. However, WEL material is not able to prevent damage to the Post-failed Carbon/Elium frame layer which has a more ductile material structure and does not cause severe damage when the supporting frame layer is damaged. The use of Post-failed Carbon/Elium as a substitute for WEL can reduce the possibility of critical injuries by 16.7% [10]. The selection of the right foam material in the helmet is also able to help absorb energy due to impact [11]. In addition to the choice of material used as the basic material for making helmets, the design and shape of the helmet greatly influence the level of safety and aerodynamic style that occurs to the rider. A good helmet has the right size for

the rider and is comfortable to wear. To create comfort for the rider, the helmet must be stable when used and not easily shaken by the wind when the rider is traveling at high speed [12]. Research on the shape of the angle of attack on the helmet has been carried out previously at angles of  $0^\circ$ ,  $10^\circ$ ,  $20^\circ$ , and  $30^\circ$ . This research was carried out on variations of the Reynolds number  $7.14 \times 10^4$ ,  $1.00 \times 10^5$ , and  $1.16 \times 10^5$  to determine the streamline of the flow that was formed while passing through the helmet surface at a certain angle of attack (AOA). The results showed that the drag force that occurred in the fluid flow across the helmet with AOA  $30^\circ$  increased. This condition can cause discomfort for cyclists because they get a fairly high resistance compared to other AOA angles [13]. By using CFD the results obtained are more effective and efficient than the experimental method [13b].

The increase in drag on the helmet with AOA  $30^\circ$  is due to the appearance of vortexes on the back of the helmet. The reduction in drag can also be done by cutting the trailing edge of the helmet which is made at the back of the helmet. Cutting the trailing edge is done to reduce the size of the vortex that appears on the back of the helmet. The study was conducted at  $Re\ 7.14 \times 10^4$ ,  $1.00 \times 10^5$  and  $1.16 \times 10^5$  by varying the trailing edge cuts at 25 mm, 75 mm and 125 mm. In general, cutting the trailing edge of the helmet can cause a decrease in the drag coefficient when used at high speeds. The results showed that a helmet with a trailing edge cut by 75 mm produced the lowest drag force when used at a high Reynolds number. However, cutting the trailing edge on the helmet is not effective at low speeds [14]. Reducing the value of the coefficient of fluid drag flowing on the helmet can also be done by adding a tail flap at the back of the helmet. The tail flap or trailing edge is the tapered back of the helmet. The addition of a bent tail flap with the right angle and height can reduce the drag coefficient value that occurs on the helmet [15].

Experimental research was also conducted to determine the effect of wind pressure on oncoming cyclists. The results showed that the front of the helmet as well as the driver's arms and elbows were exposed to the wind with higher pressure [16]. Research with 3D models can be used to describe a streamlined fluid flow across cyclists with helmets cut off from the trailing edge [17]. Helmets that have a long trailing edge do not have a vortex when used by the rider when the head is in a head-up position. However, a helmet with a trailing edge produces a vortex at the back of the rider's neck when the rider heads down. Helmets that have a trailing edge have a very aerodynamic shape resembling a drop of water. This helmet shape has a high lift coefficient and low resistance, making it more comfortable for cyclists to use.

Research conducted in 3D [17] produces a streamlined image that is almost the same as the simulation carried out in 2D [14]. Research using 2D models produces simulations with high accuracy in a shorter time. This research was conducted to simulate the streamlined shape of the fluid flow across the helmet in terms of the top section. This study was carried out as a previous development describing fluid flow across the top of the helmet ([13] & [14]). This research was carried out using a 2D model of the helmet's side-section which was simulated on Reynold Number  $7.14 \times 10^4$ ,  $1.00 \times 10^5$ , and  $1.16 \times 10^5$ . The shape of the helmet that was simulated in this study had variations on the front and this type has never been applied in other studies. In addition, in this study, variations of the Turbulence Intensity set up were 0.1%, 0.2%, and 1%. The simulation results will be shown through the value of the drag coefficient and visualization of streamlined flow.

## 2. Research Methods

This research was conducted to determine the condition of fluid flow that passes through the side cross-section of the helmet. The research was conducted using

2D numerical simulation using CFD software. The reference model used in this study is the "GIRO advantage 2 TT" time-trial helmet. The size of the "GIRO advantage 2 TT" time-trial cycling helmet simulation model is adjusted to the 2-dimensional simulation conducted by Sims, Bradford W. and Jenkins, Peter E in 2011 [18]. Furthermore, the shape of the helmet is varied into 3 types as shown in figure 1. The simulation model creation process is carried out using Solidworks 2016 Premium SP1.0 x64 software.

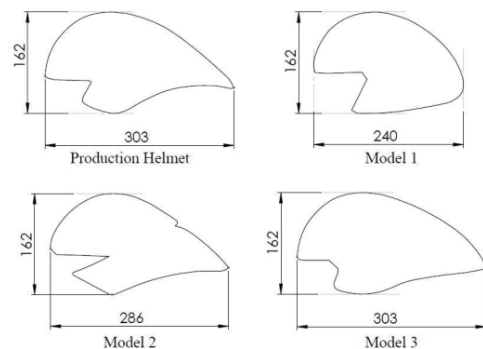


Figure 1. Helmet model simulated in this study

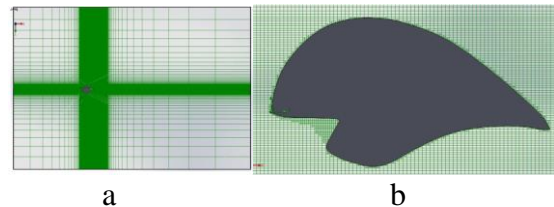


Figure 2. The mesh used in the study is in position a) the overall mesh, b) the detail of mesh on the helmet

Table 1. Set Up Boundary Condition

No	Input Parameter	Information
1	Flow type	External
2	Flow characteristics	Unsteady, Incompressible
3	Fluid	Air
4	Boundary Condition	Adiabatic wall
5	Pressure	1 atm
6	Density	1,23 kg/m <sup>3</sup>
7	Velocity	8, 11.2, 13 m/s
8	Turbulence intensity	0.1%, 0.2%, 1%
9	Turbulence model	k-ε turbulence model

Table 2. Results of research validation with differences in turbulent intensity

No	Study	Turbulent Intensity	CD	Error (%)
1	Sims dan Jenkins [18]	-	0,590	-
2	Current Study Results	0.1%	0,589	0,17
		0.2%	0,529	10,34
		1%	0,305	48,31

The simulation process begins by importing the model that has been made into CFD Solidflow software for the meshing process, determining boundary conditions, and running. The mesh used in this study is composed of submap mesh. Utilization of mesh with submap type aims to create an orderly and neat mesh structure with the optimum number of meshes. The shape of the mesh used is shown in Figure 2. To determine the optimum number of meshes, the research begins with an independent grid process. The grid independence process is carried out by running simulations on various variations in the number of meshes with the same boundary conditions. The grid independence process was carried out at Re  $1.00 \times 10^5$  with the setup boundary conditions shown in table 1. The simulation results were also validated using Sims and Jenkins research [18]. The validation process is carried out by comparing the value of the fluid flow drag coefficient with the research that is used as a reference to get the error value. The values obtained in the

grid independence process are shown in table 2.

### 3. Results and Discussion

#### 3.1 Streamline of fluid flow

The simulation of fluid flow that flows in the model is simulated at Reynolds number  $7.14 \times 10^4$ ,  $1.00 \times 10^5$ , and  $1.16 \times 10^5$ . The simulation results show a streamlined fluid flow that passes through the side cross-section of the helmet. The fluid flow contours across the simulation model form the area of a flow vortex on the back of the helmet. Oscillating Karman vortex is a phenomenon in which the fluid flow at the back of the time-trial helmet forms a repetitive vortex pattern caused by flow separation around the blunt-body. The result of the freestream simulation shown in Figure 3 is a simulation model of the helmet's side-section which was simulated at Reynolds number  $1.00 \times 10^5$ .

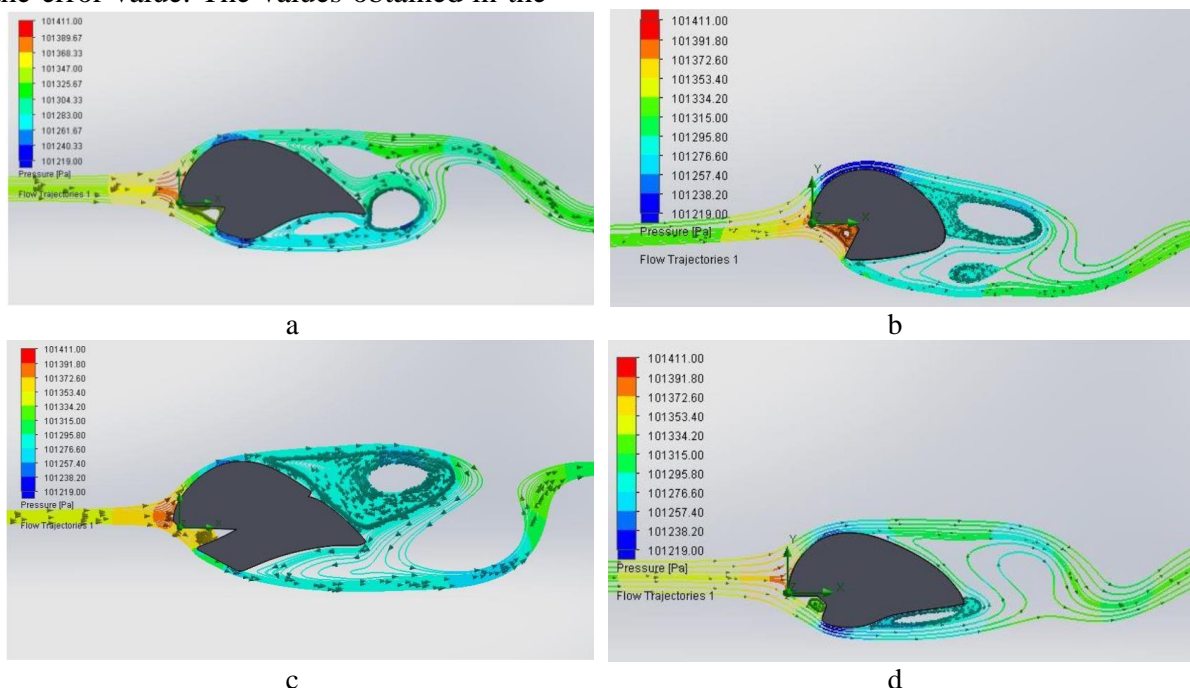


Figure 3. Streamline of fluid flow that crosses over the helmet with models a) Reference Model b) Model 1 c) Model 3 and d) Model 4

The simulation results of the helmet models that are examined each have a

different streamline. Helmet The time-trial type that is used as a reference for the

research model has the form of an Oscillating Karman vortex on the back of the helmet. The vortex appears near the trailing edge of the helmet as shown in Figure 3a. Helmet model 1 is a modified type helmet that does not have an elongated trailing edge. Helmet design model 1 is more rigid and simple for the rider. The results of the streamlined helmet 1 simulation show that the Oscillating Karman vortex appears slightly further from the back of the helmet. However, helmet design 1 has a vortex on the front of the helmet, near the temple bone. The vortex that appears on the front is quite strong, marked by a red streamlined line. Helmet model 2 has a shape that is almost similar to the time-trial type model that is used as a reference. The helmet has a long trailing edge but is equipped with shell contours. The streamline shown by the helmet simulation model 2 has an Oscillating Karman vortex on the top of the helmet. This vortex appears earlier than the time-trial type helmet that is used as a reference. The size of the vortex shown in Figure 3c on the helmet model 2 tends to be larger than the reference model. The helmet type model 3 has a shape similar to the Time trial model but with a smoother contour at the bottom. The fluid streamline

on the model 3 helmet does not produce an Oscillating Karman vortex on the back of the helmet. The vortex that is formed in this model is located at the bottom of the helmet near the rider's ear area.

### 3.2. Drag Coefficient

The formation of Oscillating Karman vortex with different sizes indicates that there are differences in the aerodynamic forces that are formed around the variation of helmet models. This vortex is formed due to the fluid flow that flows to the back of the helmet and decreases in speed so that it cannot overcome the shear stress that arises on the top surface of the helmet. This condition causes wakes to appear in areas with lower pressure. The fluid flow will experience backflow and form a layered vortex called the Oscillating Karman vortex. The area with the wake has a lower pressure compared to the fluid pressure around the helmet. The difference in pressure that occurs at the top and bottom of the helmet model will cause a drag force on the helmet. In this study, the drag force is shown through a dimensionless number in the form of the Drag Coefficient (CD). The value of the drag coefficient of each helmet model in various variations of the Reynold Number is shown in table 3.

Table 3. Drag coefficient of fluid flow across the Helmet Model at various Reynold numbers

No	Side variations	Drag Coefficient at Various Variations of Re		
		Re $7.14 \times 10^4$	Re $1.00 \times 10^5$	Re $1.16 \times 10^5$
1	<i>Production Helmet</i>	0,65	0,56	0,44
2	Model 1	1,11	0,62	0,59
3	Model 2	0,77	0,76	0,76
4	Model 3	0,57	0,51	0,38

Simulation of fluid flow across the Helmet time-trial type shows a decrease in the drag coefficient when the fluid flows with a high Reynold number. Conditions for decreasing the drag coefficient were also experienced by modified helmets 1, 2, and 3. Helmet type 1 experienced the highest decrease in drag coefficient when simulated on a high Reynold Number. The Type 1 helmet model has a greater drag coefficient than the other models on the Re  $7.14 \times 10^4$ . Type 2 helmets experience a slight decrease in drag coefficient when simulated at high Reynolds numbers. This type of helmet tends to be more stable where the drag coefficient value is approximately 0.77. Helmet model 3 has the lowest drag coefficient value when it is at Re  $1.16 \times 10^5$  which is 0.38. This condition can be explained in more detail through the flow streamline shown in Figure 5. The larger the size with the Oscillating Karman vortex that appears above the helmet, it indicates a fairly high-pressure difference between the top and bottom of the helmet. The difference in pressure on the top and bottom of the helmet causes a drag force on the vehicle. The model 3 helmet has a very low drag force because it is not formed by the Oscillating Karman vortex. The fluid flow in the model runs according to the flow model pattern. Helmet model 2 tends to be more stable when varied at various Reynold numbers. This helmet tends to be good for use in everyday conditions but still needs development to reduce the drag force that forms around the helmet.

#### 4. Conclusions

The helmet design is very influential on the aerodynamic forces caused by the fluid flowing around it. This

research was conducted on 4 variations of helmet models consisting of 1 time-trial type helmet as a reference and 3 other helmets which were developed from the basic model. The results showed that an Oscillating Karman vortex was formed at the top of the helmet due to the difference in fluid pressure on the top and bottom of the helmet. The emergence of the Oscillating Karman vortex in large size indicates the higher the drag force that occurs on the helmet. This study shows that in general, the type 1 helmet model has a larger drag coefficient than the other models at Re  $7.14 \times 10^4$ . The model 2 helmet which has a long trailing edge and shell contour produces a stable drag force for the helmet, but the drag coefficient value is still quite high, around 0.77. While the type 3 helmet with a trailing edge that is not too long and has smooth curves has the lowest drag force at Re  $1.16 \times 10^5$  with a drag coefficient value of around 0.3

#### References

- [1] Ramdani, I. (2020). Analysis of The Cycling Trend During the Pandemic of COVID 19 Towards Small and Medium Enterprises (UMKM) Income. *International Journal of Social Science and Business*, 4(4), 528–535. <https://doi.org/10.23887/IJSSB.V4I4.29610>.
- [2] Sentosa, K. W., Rahmawati, A., Arianda, D., Lahdimawan, A., & Suhendar, A. (2019). Distribution and Characteristics of Head Injury and Referral Number At Dr H. Andi Abdurrahman Noor General Hospital, Tanah Bumbu, South Borneo, Indonesia. *Neurologico Spinale Medico Chirurgico*, 1(4), 59–65. <https://doi.org/10.15562/nsmc.v1i4.1>

- [30](#).
- [3] Pedroso, F. E., Angriman, F., Bellows, A. L., & Taylor, K. (2016). Bicycle use and cyclist safety following boston's bicycle infrastructure expansion, 2009-2012. *American Journal of Public Health, 106*(12), 2171–2177. <https://doi.org/10.2105/AJPH.2016.303454>
- [4] Chiba, H., Lewis, M., Benjamin, E. R., Jakob, D. A., Liasidis, P., Wong, M. D., Navarrete, S., Carreon, R., & Demetriades, D. (2021). “Safer at home”: The effect of the COVID-19 lockdown on epidemiology, resource utilization, and outcomes at a large urban trauma center. *The Journal of Trauma and Acute Care Surgery, 90*(4), 708. <https://doi.org/10.1097/TA.00000000000003061>.
- [5] Schleinitz, K., Petzoldt, T., Kröling, S., Gehlert, T., & Mach, S. (2019). (E-)Cyclists running the red light – The influence of bicycle type and infrastructure characteristics on red light violations. *Accident Analysis & Prevention, 122*, 99–107. <https://doi.org/10.1016/j.aap.2018.11.002>.
- [6] Zainul Arifin, M., & Widyawati Agustin, I. (2018). Accident Prediction Probability Model for Cyclist in Surabaya City. *Article in Journal of Computational and Theoretical Nanoscience*. <https://doi.org/10.1166/asl.2018.11088>.
- [7] Seiniger, P., Gail, J., & Schreck, B. (2017). A draft regulation for driver assist systems addressing truck-cyclist blind spot accidents. *25th International Technical*. <https://www-esv.nhtsa.dot.gov/Proceedings/25/25E SV-000198.pdf>
- [8] Baschera, D., Lawless, A., Roeters, R., Frysch, C. W. S., & Zellweger, R. (2020). Severity and predictors of head injury due to bicycle accidents in Western Australia. *Acta Neurochirurgica 2020 163:1, 163*(1), 49–56. <https://doi.org/10.1007/S00701-020-04626-W>
- [9] Hoye, A. (2018). Recommend or mandate? A systematic review and meta-analysis of the effects of mandatory bicycle helmet legislation. *Accident Analysis & Prevention, 120*, 239–249. <https://doi.org/10.1016/j.aap.2018.08.001>
- [10] Gohel, G., Bhudolia, S. K., Elisetty, S. B. S., Leong, K. F., & Gerard, P. (2021). Development and impact characterization of acrylic thermoplastic composite bicycle helmet shell with improved safety and performance. *Composites Part B: Engineering, 221*, 109008. <https://doi.org/10.1016/j.compositescb.2021.109008>
- [11] Mustafa, H., Pang, T. Y., Ellena, T., & Nasir, S. H. (2019). Impact attenuation of user-centred bicycle helmet design with different foam densities. *Journal of Physics: Conference Series, 1150*(1), 012043. <https://doi.org/10.1088/1742-6596/1150/1/012043>
- [12] Pang, T. Y., Lo, T. S. T., Ellena, T., Mustafa, H., Babalija, J., & Subic, A. (2018). Fit, stability and comfort assessment of custom-fitted bicycle helmet inner liner designs, based on 3D anthropometric data. *Applied Ergonomics, 68*, 240–248. <https://doi.org/10.1016/j.apergo.2017.12.002>.
- [13] Syafik, H. M., & Putro Iswanto, Y. (2018). Study the effect of angle of attack on flow characteristics atracing bike helmet using CFD. <https://doi.org/10.1051/mateconf/201820406001>.
- [13b] Syamsuri, Chern MJ, Vaziri N. (2022). SPH Model For Interaction Of Sloshing Wave With Obstacle In Shallow Water Tank, *Journal of King*

- Saud University - Engineering Sciences 34 (2), 126-138.
- [14] Syamsuri, S., Novianarenti, E., & Huda, K. (2018). The Influence Of Length Cuts Trailing Edge On Flow Characteristics In The Railway Helm Using Computational Fluid Dynamics. *VANOS Journal of Mechanical Engineering Education*, 3(1).  
<https://jurnal.untirta.ac.id/index.php/vanos/article/view/3370>
- [15] Kamarudin, K. M., Basri, M. S. M., Maidin, N. A., & Rahman, M. H. A. (2020). Aerodynamic Drag Study of Time-Trial Cycling Helmets Using CFD Analysis. *Journal of Advanced Research in Fluid Mechanics and Thermal Sciences*, 72(1), 21–31.  
<https://akademiabaru.com/submit/index.php/arfmts/article/view/2993>
- [16] Giappino, S., Omarini, S., Schito, P., Somaschini, S., Belloli, M., & Tenni, M. (2018). Cyclist Aerodynamics: A Comparison Between Wind Tunnel Tests and CFD Simulations for Helmet Design. *Lecture Notes in Civil Engineering*, 27, 336–349.  
[https://doi.org/10.1007/978-3-030-12815-9\\_27](https://doi.org/10.1007/978-3-030-12815-9_27).
- [17] Beaumont, F., Taiar, R., Polidori, G., Trenchard, H., & Grappe, F. (2018). Aerodynamic study of time-trial helmets in cycling racing using CFD analysis. *Journal of Biomechanics*, 67, 1–8.  
<https://doi.org/10.1016/J.JBIOMECH.2017.10.042>.
- [18] Sims, B. W., & Jenkins, P. E. (2012). Aerodynamic Bicycle Helmet Design Using a Truncated Airfoil With Trailing Edge Modifications. *ASME 2011 International Mechanical Engineering Congress and Exposition, IMECE 2011*, 6(PARTS A AND B), 453–462.  
<https://doi.org/10.1115/IMECE2011-65411>